

Clark University

## Clark Digital Commons

---

Geography

Faculty Works by Department and/or School

---

2022

### Applying landscape fragmentation analysis to icescape environments: potential impacts for the Pacific walrus (*Odobenus rosmarus divergens*)

Anthony Himmelberger  
*Clark University*

K E. Frey  
*Clark University, [kfrey@clarku.edu](mailto:kfrey@clarku.edu)*

Florencia Sangermano  
*Clark University*

Follow this and additional works at: [https://commons.clarku.edu/faculty\\_geography](https://commons.clarku.edu/faculty_geography)



Part of the [Geography Commons](#)

---

#### Repository Citation

Himmelberger, Anthony; Frey, K E.; and Sangermano, Florencia, "Applying landscape fragmentation analysis to icescape environments: potential impacts for the Pacific walrus (*Odobenus rosmarus divergens*)" (2022). *Geography*. 26.

[https://commons.clarku.edu/faculty\\_geography/26](https://commons.clarku.edu/faculty_geography/26)

This Article is brought to you for free and open access by the Faculty Works by Department and/or School at Clark Digital Commons. It has been accepted for inclusion in Geography by an authorized administrator of Clark Digital Commons. For more information, please contact [larobinson@clarku.edu](mailto:larobinson@clarku.edu), [cstebbins@clarku.edu](mailto:cstebbins@clarku.edu).

## RESEARCH ARTICLE

# Applying landscape fragmentation analysis to icescape environments: potential impacts for the Pacific walrus (*Odobenus rosmarus divergens*)

Anthony Himmelberger, Karen E. Frey &amp; Florencia Sangermano

Graduate School of Geography, Clark University, Worcester, MA, USA

## Abstract

Sea-ice cover across the Arctic has declined rapidly over the past several decades owing to amplified climate warming. The Pacific walrus (*Odobenus rosmarus divergens*) relies on sea-ice floes in the St. Lawrence Island (SLI) and Wainwright regions of the Bering and Chukchi seas surrounding Alaska as a platform for rest, feeding and reproduction. Lower concentrations of thick ice floes are generally associated with earlier seasonal fragmentation and shorter annual persistence of sea-ice cover, potentially affecting the life history of the Pacific walrus. In this study, 24 Landsat satellite images were classified into thick ice, thin ice or open water to assess sea-ice fragmentation over the spring-summer breakup period. Geospatial fragmentation analyses traditionally used in terrestrial landscapes were newly implemented in this study to characterize the icescape environment. Fragmentation of sea ice was assessed based on the Percent of Landscape, Number of Patches, Mean Area, Shape Index, Euclidean Nearest Neighbor and Edge Density. Results show that lower sea-ice concentrations in both the SLI and Wainwright regions were associated with smaller sea-ice floes. In the Bering Sea, lower sea-ice concentrations were also associated with increases in the number of ice floes, floe isolation and edge density. By contrast, lower sea-ice concentrations in the Chukchi Sea were associated with ice floes that were more circular in shape. The continuation of sea-ice decline with shifting icescape characteristics may result in walruses having to swim longer distances in the northern Bering Sea and adapt to use less-preferred, rounder ice floes in the Chukchi Sea.

## Keywords

Cryosphere; climate change; sea ice; remote sensing; Landsat; sea ice-obligate species

## Correspondence

Karen E. Frey, Graduate School of Geography, Clark University, 950 Main Street, Worcester, MA 01610, USA.  
E-mail: kfrey@clarku.edu

## Abbreviations

ENN: Euclidean Nearest Neighbor (distance), metric in the FRAGSTATS software programme  
LiDAR: light detection and ranging (remote sensing)  
SAR: synthetic aperture radar  
SIC: sea-ice cover  
SLI: St. Lawrence Island, Alaska

To access the supplementary material, please visit the article landing page

## Introduction

The impacts of climate change in the Arctic are drastic, with surface air temperatures warming at twice the global average rate (Overland et al. 2018). Warming air temperatures are causing SIC to decline precipitously: the 13 lowest sea-ice concentrations in the satellite record dating back to 1972 occurred in the last 13 years (Perovich et al. 2019), and some estimates project that the Arctic will be ice-free by the summer of 2040 (Hauser et al. 2018). Since 2007, the summer sea-ice edge in the Chukchi Sea has retreated more than 300 km farther north than the previous 30-year average (Battaile et al. 2017). The

overall extent of September SIC across the pan-Arctic has retreated by 14% per decade (Hauser et al. 2018), and the Arctic-wide melt season has lengthened at a rate of five days per decade from 1979 to 2013 (Strove et al. 2014). Additionally, ice-albedo feedbacks will enhance sea-ice decline by hastening melting over the coming decades and leading to a much shorter ice season in the Arctic. Sea-ice types and their description based on available literature are defined in Table 1 (Burns et al. 1980; Ray & Hufford 1989; Ray et al. 2010).

The decline of sea-ice impacts Arctic inhabitants, including the Pacific walrus (*Odobenus rosmarus divergens*). The Pacific walrus represents about 90% of all walruses

**Table 1** Sea-ice attributes based on available literature. Categories and definitions are taken from Burns et al. (1980), Ray & Hufford (1989) and Ray et al. (2010).

| Sea-ice type                    | Description  |
|---------------------------------|--|
| Continuous pack/heavy ice cover | Continuous ice with no visible leads.  |
| Pack ice with leads (cracks)    | The first stage of breaking of continuous ice cover; when pack ice is crossed by leads that are generally sub-parallel and may intersect.                            |
| Broken pack                     | Two or more intersecting sets of leads forming floes of various sizes. Ice is dispersed enough so that open water and thin ice are also available (Ray et al. 2010). |
| Rounded pack                    | Areas of at least 50% heavy ice cover; the floes are rounded rather than angular.  |
| Loose pack                      | Areas of less than 50% heavy ice cover, consisting of scattered floes.   |

worldwide, all of which reside in the Arctic (Fischbach et al. 2016) and were recently denied endangered or threatened status under the US Endangered Species Act (US Fish & Wildlife Service 2017). Sea ice is a vital aspect of the Pacific walrus habitat. It is used as a resting, birthing and nursing platform, providing access to offshore feeding areas and refuge from predators and other disturbances (Monson et al. 2013). Although walruses can dive more than 250 m deep, they do not usually feed at more than 80 m depth (Fay 1982; Jay & Fischbach 2008). As sea-ice extent decreases, the ice pack terminates over deeper water north of the shelf break, preventing walruses from conveniently accessing the shallower waters where they usually feed (Taylor et al. 2018). Overall declines in sea-ice extent and quantity have increasingly forced walruses (including adult females and young) to retreat to coastal haul-outs to rest. This behaviour creates abnormally crowded environments (Jay et al. 2011) that can be dangerous, particularly for young calves (Wartzok & Ray 1980; Monson et al. 2013). Walruses are also likely forced to swim away from sea-ice floes owing to increases in human use of the seascape (MacCracken 2012; McFarland & Aerts 2015). Ship traffic in the region has doubled between 2010 and 2017 (Miller 2015), with estimates that by mid-century, the length of the navigable open water season will also double (Melia et al. 2016), further encouraging the use of coastal haul-outs.

This study is novel because it uses the methodology traditionally used in landscape fragmentation analysis to assess an icescape. Fragmentation, or the process by which a landscape is broken into smaller homogeneous areas, or patches, is a critical measure of habitat quality since it impacts how species use and move within the landscape (Turner et al. 2003). More specifically, the

process of fragmentation divides large, continuous habitats into smaller, more isolated fragment patches (Didham 2010). Studies of landscape fragmentation have been conducted since the early 1990s, primarily to analyse forest and other habitats (Franklin & Foreman 1987; Saunders et al. 1991; Baker & Cai 1992; Reed et al. 1996; Hargis et al. 1998). Habitat fragmentation analyses are rarely applied to marine-based icescapes. Icescapes are far more temporally complex than landscapes since sea ice changes and moves frequently, making it challenging to compare across different years, months, days or even hours. To our knowledge, only two other studies have implemented fragmentation analysis of sea ice. One assessed polar bear habitat using 25 km resolution satellite imagery (Sahanatien et al. 2012). We advance upon this previous research by using higher spatial resolution imagery, examining multiple fragmentation metrics and analysing how they correlate with SIC specifically. The other study focused on assessing walrus occupancy in the Bering Sea, using SAR imagery and aerial photography, with limitations in the extent of the study area and resolution: SAR imagery, with a 100 m resolution in this case, could only identify two classes of seascape: fragmented pack and ocean/ice (Sacco 2015). Our analysis fills gaps in the Sacco (2015) study by using satellite imagery to cover a larger geographic extent at a higher spatial resolution. The methods used in this study demonstrate how terrestrial habitat fragmentation analysis can be applied to future analyses of sea icescapes.

The objectives of this study were to (1) assess the general fragmentation characteristics of sea ice in walrus habitat, (2) compare sea-ice characteristics in the Chukchi versus Bering Sea regions of Alaska (two contrasting locations selected for their high distribution of walrus population during different times of the year), (3) examine how these spatial pattern metrics vary across high and low sea-ice concentrations and (4) use these results to infer how future fragmentation characteristics of sea-ice habitat may impact the life history of the Pacific walrus.

## Data and methods

### Study area

This study compares two Arctic regions: (a) south-east of SLI in the northern Bering Sea and (b) north and north-west of Wainwright, Alaska, in the Chukchi Sea. These locations were chosen because of their high distribution of walruses based on satellite tagging data acquired from Citta et al. (2018), other satellite tagging studies (Jay et al. 2012), Pacific walrus behaviour modelling studies (Udevitz et al. 2017) and data acquisition limitations (see a later section). The Pacific walrus

population is located in the northern Bering Sea, south of SLI (Oakley et al. 2012), during the mating season in January, February and early March (Jay et al. 2011). In late spring (April–June), females begin calving and follow the sea ice as it recedes northward to the Chukchi Sea (Jay et al. 2011; Monson et al. 2013). At the same time, male walrus begin to haul out on coastal land to rest between feeding trips in the Bering Sea and the northern coast of Chukotka; they are increasingly joined by females and young in the summer months as SIC declines (Jay et al. 2011).

We defined the Bering Sea region south-east of SLI as the intersection of Landsat path 81/row 16 and path 82/row 16 scenes (approximately 19 859 km<sup>2</sup>; Fig. 1a). This area of the Bering Sea is known for being highly dynamic and varies in sea-ice patch concentration both seasonally and interannually (Ray et al. 2016). Just south of the island is the SLI Polynya, which often extends the entire length of the island (150 km) and can reach as far as 25 km offshore (Jay et al. 2010). The formation of the polynya is very important for walrus as it continuously

creates new ice, while an area of open water—giving the walrus access the seafloor to feed—often remains (Burns et al. 1980; McNutt 2002). This area is known for having large distributions of walrus throughout the winter months (December–April; Drucker et al. 2003), with more recent studies pinpointing walrus to be more abundant west of the SLI Polynya, towards Russia (Ray et al. 2016; Citta et al. 2018). Over the past decade, there have been substantial decreases in the annual persistence of SIC in the Bering Sea. The ice extent in the northern Bering Sea during February–March 2018 and 2019 was the lowest on record, owing largely to the increased occurrence of warm, southerly winds, pushing ice floes to the north (Frey et al. 2019; Stabeno & Bell 2019; Stabeno et al. 2019). Southerly winds, coupled with an expected increase in wave intensity and storm frequency (Bateson et al. 2020), lead to an enhanced lateral melt rate and may likely continue to contribute to decreasing sea-ice annual persistence in this region into the future. The observation by Ray et al. (2016) that as SIC declines, sea-ice dynamics transition from a ‘plastic continuum’

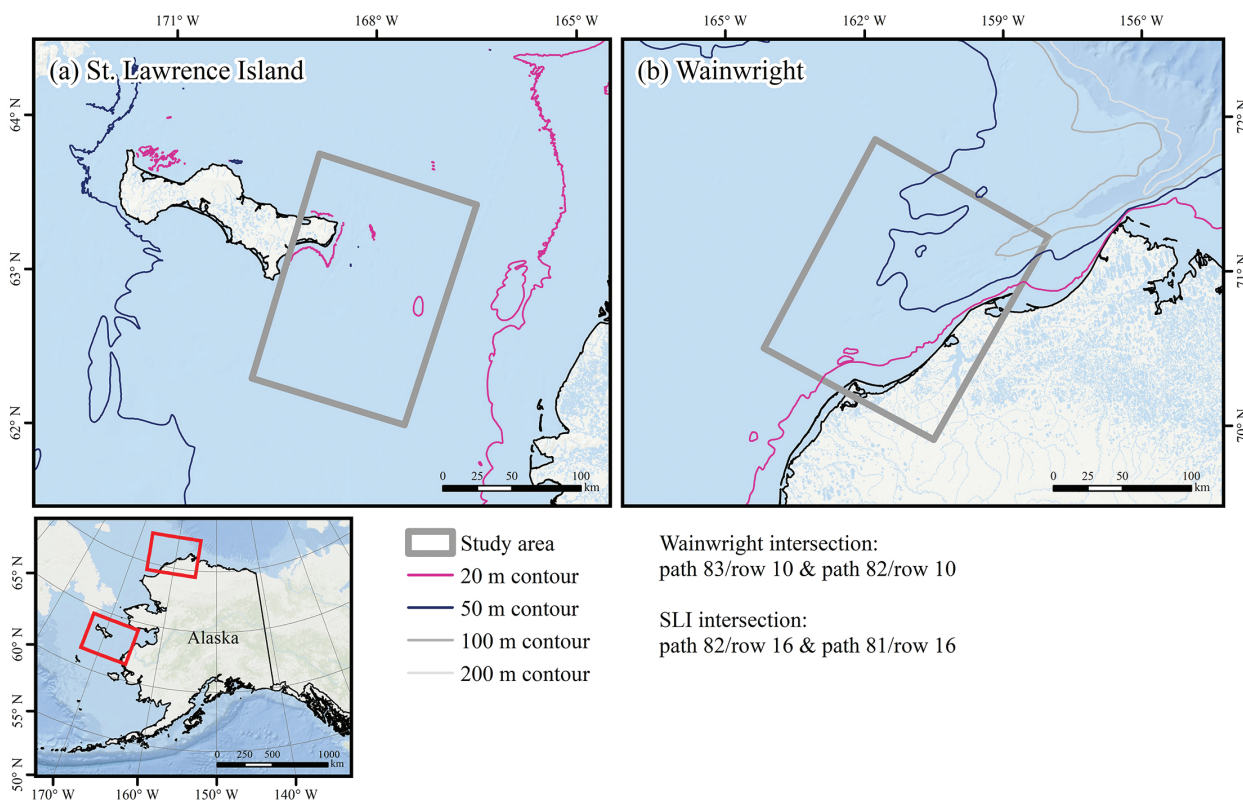


**Fig 1** Study area map of locations in Alaska: (a) area south-east of SLI, intersection of Landsat path 81/row 16 scene and path 82/row 16 scene (approximately 19 859 km<sup>2</sup>); (b) the area north of Wainwright, AK, intersection of Landsat path 82/row 10 and path 81 path/row 10 scenes (about 22 577 km<sup>2</sup>). Bathymetry data accessed from the US Geological Survey (Schumacher 1976a, b).

(dictated by fracture mechanics) to a pattern of independently moving ice floes may, therefore, become far more common with climate change. These scenarios are referred to as a ‘mixing bowl’ of groupings of varying floe sizes and thickness and may make it more challenging to distinguish between different types of sea-ice pack classifications in the future.

We defined the Chukchi Sea study region over Hanna Shoal (north and northwest of Wainwright, Alaska) as the intersection of Landsat path 82/row 10 and path 81 path/row 10 scenes (ca. 22 577 km<sup>2</sup>; Fig. 1b). Historically, there has been high walrus activity in this area during the summer and fall, although this has been decreasing as the lack of sea ice makes it less feasible for walruses to reach Hanna Shoal (Jay et al. 2012). In spring 2019, sea ice in Chukchi Sea melted 20–35 days earlier than the 1981–2010 average, which led to record low SIC until early August (Perovich et al. 2019). Continued reduction in the sea-ice season is expected in the coming decades. Some models suggest that by the end of the century, the Chukchi Sea will experience sea-ice break-up one month earlier in the spring and freeze-up two months later in the fall (Jay et al. 2012). New ice formation occurring later in the season followed by earlier melt would cause sea-ice fragmentation during July, with ice-free conditions during August, September and October rather than just September (Douglas 2010; Jay et al. 2011). Additionally, sea-ice fragmentation in the Chukchi Sea has retreated north of the continental shelf during eight out of the last 10 years (Udevitz et al. 2017). As these trends continue, compact sea ice will become less available for walruses owing to southerly winds pushing sea ice farther away from potential feeding areas (Perovich et al. 2019).

Mean daily sea-ice climatologies and time series of annual sea-ice persistence were investigated based on data from Comiso et al. (Comiso, Gersten et al. 2017; Comiso, Meier et al. 2017) to understand better the differences in sea-ice dynamics for the Bering and Chukchi seas study areas. Both data sets were extracted for each study area, and trend lines in SIC over 2008–2018 were calculated (not shown). The Wainwright study area is typically covered in ice from mid-November to mid-June, whilst the annual persistence has decreased from more than 300 days of ice cover in the 1980s to mid-1990s to just ca. 225 in the past decade, losing approximately 31 days of SIC per decade. Sea ice around the SLI study area is similar, with consistently high volumes from December to April. SLI has lost 8 days of SIC per decade, with just over 100 days of annual persistence in 2018, whereas from the 1980s to 2010, sea-ice persistence was relatively stable and lasted approximately 175 days per year.

**Data collection and processing**

This study used Landsat 5 Thematic Mapper and Landsat 8 Operational Land Imager data collected through EarthExplorer, a US Geological Survey data portal for obtaining satellite imagery. Owing to the Scan Line Corrector issue, Landsat 7 ETM+ Satellite Sensor data were deemed unusable (USGS 2017). Images were collected from February to May for the SLI region, as more extensive sea ice during the winter months begins to break up throughout spring. Images for the Wainwright region were collected from March to July as sea-ice break-up occurs two months later than in the SLI region. Twenty-four images were analysed: 14 for the SLI region and 10 for the Wainwright region (Table 2), spanning from February to July of 2008 to 2018. Data pre-processing was performed using both TerrSet and ArcMap 10.6. Study areas were defined by intersecting the extent of Landsat scenes (two adjacent scenes per study location; USGS 2018), and land areas were excluded from the analysis.

**Table 2** Summary table of all SLI and Wainwright Landsat images, in chronological order.

| Date       | Path/row | Landsat 5/8 |
|------------|----------|-------------|
| SLI        |          |             |
| 1-May-09   | 82/16    | 5           |
| 29-Mar-11  | 81/16    | 5           |
| 14-Apr-11  | 81/16    | 5           |
| 5-Apr-13   | 82/16    | 8           |
| 19-Apr-13  | 81/16    | 8           |
| 8-Feb-14   | 82/16    | 8           |
| 21-Mar-14  | 81/16    | 8           |
| 11-Feb-15  | 82/16    | 8           |
| 15-Mar-15  | 82/16    | 8           |
| 16-Apr-15  | 82/16    | 8           |
| 17-Mar-16  | 82/16    | 8           |
| 26-Mar-16  | 81/16    | 8           |
| 30-Apr-17  | 81/16    | 8           |
| 3-Feb-18   | 82/16    | 8           |
| Wainwright |          |             |
| 21-May-08  | 83/10    | 5           |
| 21-Mar-09  | 83/10    | 5           |
| 6-Apr-09   | 83/10    | 5           |
| 24-May-09  | 83/10    | 5           |
| 9-Jul-14   | 83/10    | 8           |
| 19-Jun-15  | 82/10    | 8           |
| 5-Jul-15   | 82/10    | 8           |
| 15-Jun-17  | 83/10    | 8           |
| 15-Apr-18  | 83/10    | 8           |
| 13-Jul-18  | 82/10    | 8           |

**Table 3** Error matrix comparing segmentation classification across all images with manual classification. Rows represent segmentation classification, and columns represent the reference classification. Overall accuracy is 90.75%.

|                                | Overall summary |          |       |       | User's accuracy (%) | Commission error (%) |
|--------------------------------|-----------------|----------|-------|-------|---------------------|----------------------|
|                                | Thick ice       | Thin ice | Water | Total |                     |                      |
| Thick ice                      | 455             | 38       | 1     | 494   | 92.11               | 7.89                 |
| Thin ice                       | 15              | 255      | 10    | 280   | 91.07               | 8.93                 |
| Water                          | 0               | 47       | 379   | 426   | 88.97               | 11.03                |
| Total                          | 470             | 340      | 390   | 1200  |                     |                      |
| Producer's accuracy (%)        | 96.81           | 75.00    | 97.18 |       |                     |                      |
| Omission error (%)             | 3.19            | 25.00    | 2.82  |       |                     |                      |
| Total correct reference points | 1089            |          |       |       |                     |                      |
| Total 'true' reference points  | 1200            |          |       |       |                     |                      |
| Percent accuracy               | 90.75           |          |       |       |                     |                      |

### Classification of sea ice

This study used a combination of object-based and unsupervised classification methods to define sea-ice patch concentrations. A histogram peak unsupervised classification was used to distinguish between spectrally different classes of sea ice and water (Eastman 2016). For Landsat 8 scenes, all spectral bands 1 through 7 were used in the classification, whereas for Landsat 5, all bands were used, excluding the thermal band. The maximum number of clusters parameter was set to three, as this setting could consistently separate thick ice, thin ice and water across all scenes. Ocean water and thick ice are the most important for walrus, as the former is their medium for swimming and feeding, while the latter is ideal for hauling out and resting. Ice that is sufficiently thin for walrus to create breathing holes from beneath the ice would not support the weight of a walrus attempting to rest (Kastelein et al. 1991; Ray et al. 2010; Jay et al. 2011). However, thin ice was included in the classification for spectral class completeness, allowing better separation of thick ice and water. Segmentation classification, which groups neighbouring pixels into segments or patches, was employed to classify the icescape according to the similarity between their spectral characteristics. The final sea-ice classification was generated by assigning to each segment the category (thick ice, thin ice or water) that was most prevalent within it. Segmentation classification can improve the accuracy of the pixel-based classification and produce a smoother result that preserves boundaries between segments (Hisabayashi et al. 2017) and is well suited for this study that focuses on the fragmentation of individual sea-ice floes.

The accuracy of each final classified image was assessed by creating 50 stratified random data points for each image and evaluating each point through visual inspection using the corresponding true colour composite image. Classes visually interpreted from the true colour

composite were considered the reference class. An error matrix was created for each image, identifying the frequency of evaluation points that corresponded (or not) with the reference class. A summary accuracy matrix across all 24 images was also calculated (Table 3).

### Icescape structure

The FRAGSTATS version 4.2 software was used to assess the general fragmentation characteristics of sea-ice patches and compare the icescape structure characteristics in the Chukchi versus Bering Sea regions of Alaska. Only thick ice can support walrus haul-outs; therefore, this class alone was input into the fragmentation analysis software. Six metrics were used to assess the icescape structure: (a) Percent of Landscape, (b) Number of Patches, (c) Mean Patch (i.e., ice floe) Area (hectares), (d) Shape Index, (e) ENN (m) and (f) Edge Density (metres of edge per hectare of ice). Percent of Landscape represents the percent of the image covered in thick ice, with decreases indicating loss of SIC. Number of Patches is the total number of individual thick-ice floes within each image, with higher numbers indicating a more fragmented landscape. Mean Patch Area is the total area of all ice floes (in m<sup>2</sup>), divided by the number of floes and divided by 10 000 (to convert to hectares), representing the average size of a thick-ice floe. Shape Index is the ice floe perimeter divided by the square root of ice floe areas, indicating the roundness of thick ice walrus habitat. This metric was chosen instead of the perimeter–area ratio because it is standardized to account for the size of the ice floe. A visual example of the Shape Index can be seen in Fig. 2. ENN is equal to the distance (m) of the nearest thick-ice floe based on the shortest edge-to-edge-distance, indicating isolation of sea-ice floes. Edge Density is the sum of the lengths of all thick ice edge segments, divided by the total landscape area, multiplied by 10 000 (hectares; McGarigal 2015) and

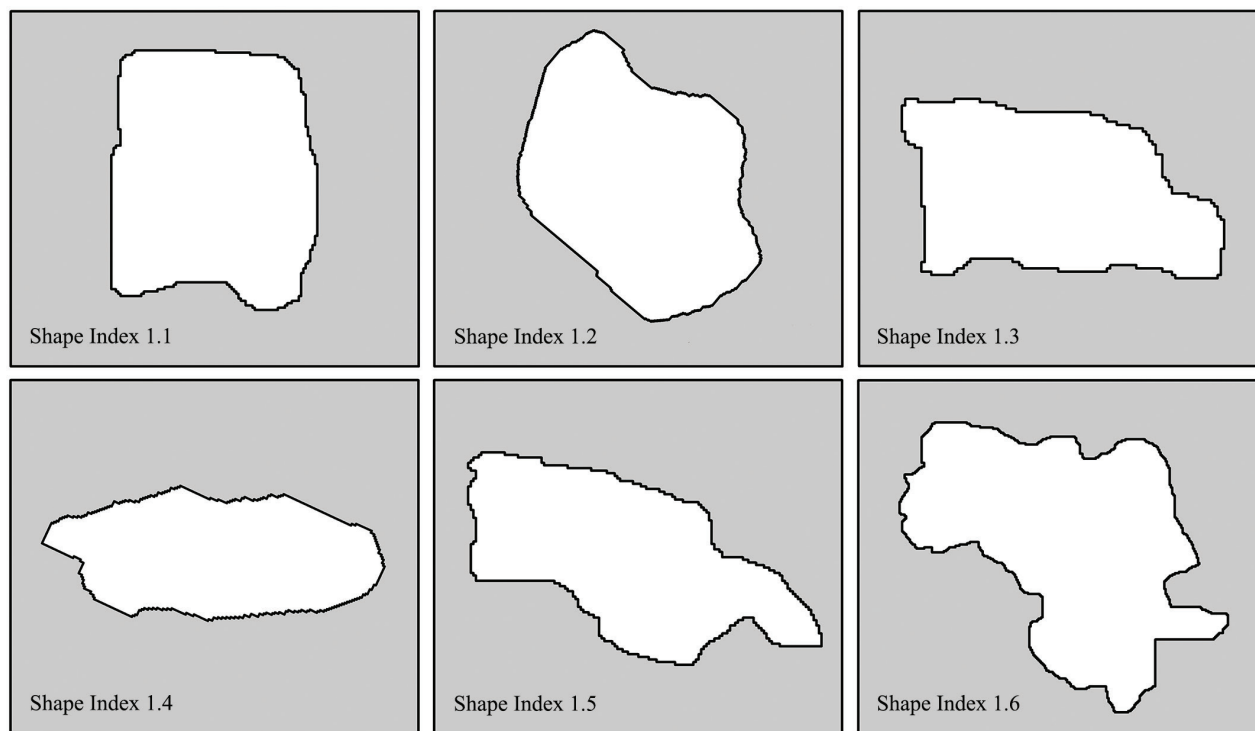


**Fig 2** Example sea-ice floes visualizing the shape index metric.

divided by sea-ice concentration to normalize this metric. See Supplementary Table S1 for a more detailed explanation of why each metric was chosen for our analysis. Each fragmentation metric was plotted against SIC to allow comparisons across scenes of different sea-ice coverages, and account for limited data. Plotting fragmentation metrics versus time was not feasible in this study as the temporal resolution of the data did not allow for the use of the data to show change over a multi-year time series.

### Limitations

We do note that Landsat imagery was still somewhat limiting. Few images within a year were available for the classification of sea-ice habitat, owing to the 16-day temporal resolution of the satellite, prevalent cloud cover and variability of daylight length within the study area. Moreover, images acquired from the Landsat 7 ETM+ sensor were also deemed unusable owing to the Scan Line Corrector failure, which substantially decreased the temporal resolution of our data set. These limitations are similar to another sea-ice study that compared Landsat and MODIS satellites, finding similar temporal resolution limitations of the two (Rösel & Kaleschke 2011). Although the 30 m resolution of Landsat gives a general representation of the seascape, sea-ice floes can be smaller than 30 m, and it is not uncommon for walruses to utilize smaller floes (Fay et al. 1984).

This spatial resolution limitation could result in the underestimation of floes, as floes smaller than 30 m may have been identified as water or thin-ice using our classification. Higher spatial resolution imagery would remove this uncertainty and give an improved synopsis of patch dynamics between extremely small ice floes, at the expense of temporal and geographic coverage. However, the advantage is that Landsat data have the longest record of mid-resolution imagery dating back to 1972, allowing our analysis to extend temporally farther than other satellites. We also would like to acknowledge that this analysis does not consider other important sea-ice characteristics, such as surface roughness owing to the two-dimensional nature of our satellite imagery; future studies could utilize LiDAR to incorporate these. Also, our analysis only focuses on sea-ice patch dynamics. Other sea-ice habitat features such as intersecting leads are omitted from this study, but we acknowledge their importance for future studies.

### Results

The overall accuracy of the segmentation classification images was 90.75% (Table 3), with Wainwright having slightly higher accuracy than SLI (91.40 and 90.29%, respectively). Additionally, thick ice was classified with an omission error of 3.19%. The most common error was

classifying thin ice as water (4% of evaluation points). This error is attributed to the high variability in the thickness of sea ice. Since fragmentation was assessed for thick ice, these errors do not affect the results of our study. The other common error was classifying thin ice as thick ice (3% of evaluation points), which may have slightly impacted the results of this study. To further examine the accuracy

assessment, the model only misclassified one point of water as thick ice and did not classify any thick ice as water. This demonstrates that the classification did a robust job differentiating between water and thick ice (the two more important categories for this study). Two true colour composite and classification examples were chosen to illustrate high and low sea-ice concentrations (Figs. 3, 4).

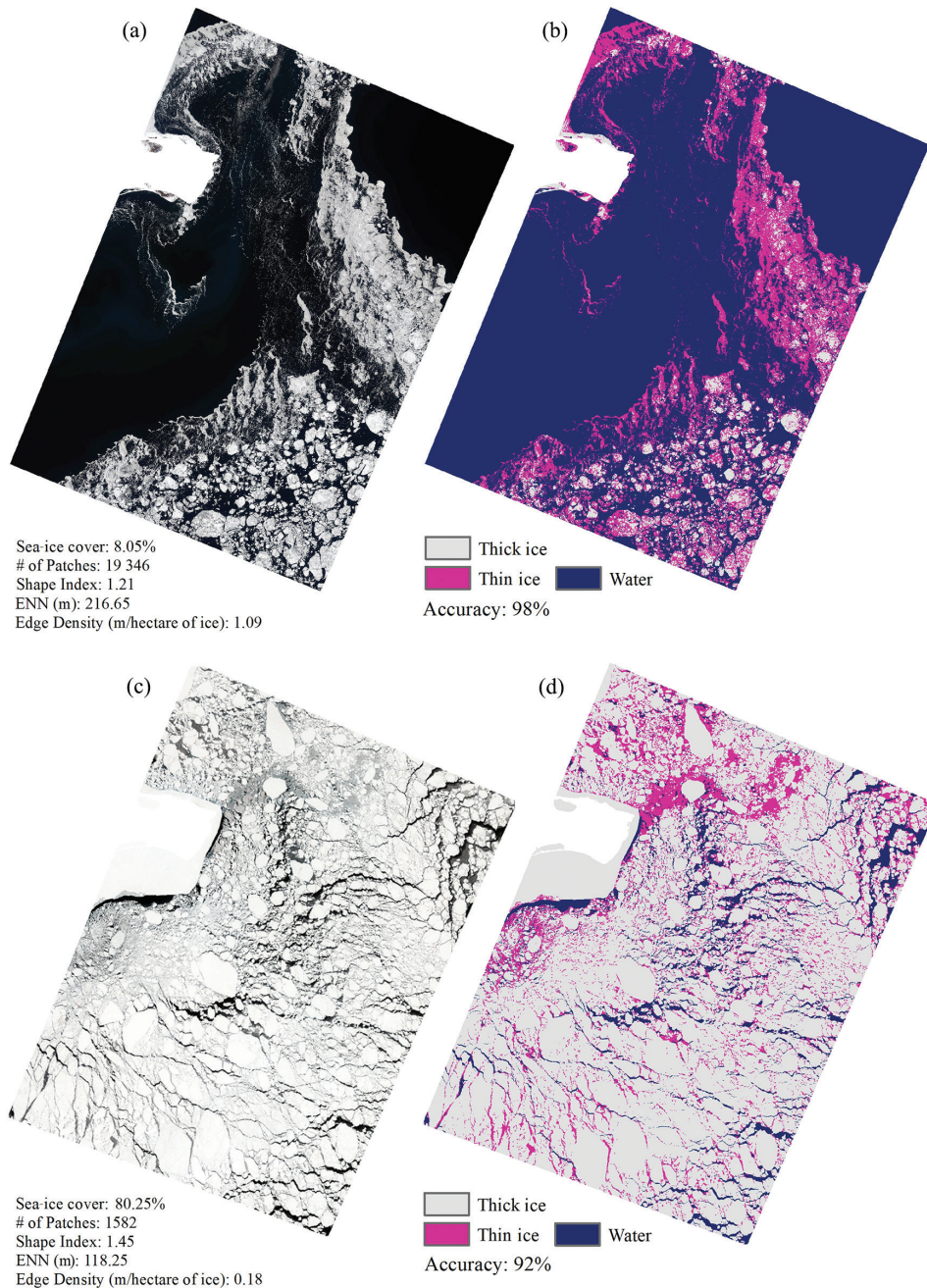


**Fig 3** Comparison of cluster classification to true colour composite images: (a) true colour composite from the SLI study area, 30 April 2017; (b) segmentation classification of 30 April 2017 image (accuracy: 98%); (c) true colour composite from SLI study area, 29 March 2011; and (d) segmentation classification of 29 March 2011 image (accuracy: 92%).



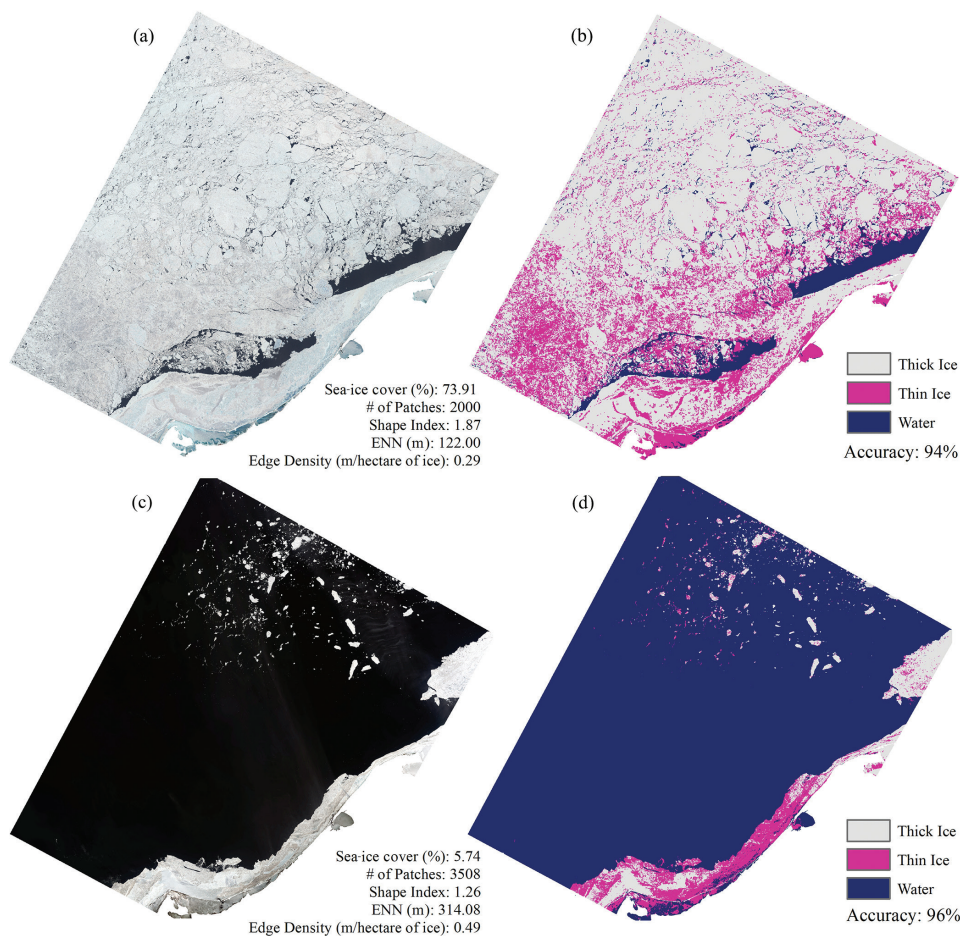


**Fig 4** Comparison of cluster classification to true colour composite images: (a) true colour composite from Wainwright study area, 24 March 2009; (b) segmentation classification of 24 March 2009 image (accuracy: 94%); (c) true colour composite from Wainwright study area, 15 June 2017; and (d) segmentation classification of 15 June 2017 image (accuracy: 96%).

Classified images for sea-ice concentration ranged 1.7–80.25%, giving large variation in the outputs for all other metrics (Table 4). Six of the 10 correlations tested were statistically significant (Table 5). The Number of Patches in SLI presented the most significant negative correlation with SIC ( $R = -0.88$ ,  $p < 0.01$ ; Fig. 5a). As sea ice decreased from about 80% to about 15%, the number of ice floes increased by 650% (from ca. 2000 to ca. 15 000 ice floes), indicating a more fragmented icescape. The Mean Patch Area in SLI had a significant positive correlation with SIC ( $R = 0.86$ ,  $p < 0.01$ ; Fig. 5b), indicating a decrease in the size of sea-ice floes with declining sea-ice concentration. ENN had a significant negative correlation with SIC ( $R = -0.77$ ,  $p < 0.01$ ; Fig. 5d). Distances from floe to floe increased from ca. 140 m to ca. 200 m as sea-ice coverage decreased from about 80% to about 15%, an increase of 43%, indicating a rise in sea-ice floe isolation with the decline of sea ice. Edge

density in SLI was significantly negatively correlated with SIC ( $R = -0.86$ ,  $p < 0.01$ ; Fig. 5e). As SIC decreased from about 80% to about 15%, Edge Density increased by 200%, from ca. 0.2 to ca. 0.6 hectares/SIC, indicating an increase in thick-ice fragmentation with declines in sea ice. Only two metrics were statistically significant for Wainwright: Mean Area and Shape Index. Mean Area was significantly positively correlated with SIC ( $R = 0.79$ ,  $p < 0.01$ ; Fig. 5g) as was Shape Index ( $R = 0.85$ ,  $p < 0.01$ ; Fig. 5h). The Shape Index decreased from ca. 1.8 to ca. 1.2, or 33%, as sea-ice coverage decreased from about 75% to about 5%, indicating more compact/circular ice floes.

## Discussion

Our analyses indicate that the Chukchi and Bering seas of Alaska have likely experienced shifts in sea-ice

**Table 4** FRAGSTATS output for each image in SLI and Wainwright, ordered chronologically.

| Date       | SIC (%) | Number of patches | Mean area (hectares) | Shape index | ENN (m) | Edge density (m per hectare of ice) |
|------------|---------|-------------------|----------------------|-------------|---------|-------------------------------------|
| SLI        |         |                   |                      |             |         |                                     |
| 1-May-09   | 45.32   | 5927              | 143.43               | 1.54        | 160.65  | 0.3                                 |
| 29-Mar-11  | 80.25   | 1582              | 955.02               | 1.45        | 118.25  | 0.18                                |
| 14-Apr-11  | 62.41   | 2163              | 546.4                | 1.51        | 140.9   | 0.18                                |
| 5-Apr-13   | 63.59   | 3562              | 342.65               | 1.29        | 142.97  | 0.12                                |
| 19-Apr-13  | 57.69   | 4645              | 237.79               | 1.23        | 199.08  | 0.18                                |
| 8-Feb-14   | 36.22   | 14 208            | 49.16                | 1.33        | 148.56  | 0.39                                |
| 21-Mar-14  | 61.78   | 5671              | 211.34               | 1.27        | 137.77  | 0.19                                |
| 11-Feb-15  | 41.58   | 9462              | 85.24                | 1.34        | 163.48  | 0.29                                |
| 15-Mar-15  | 57.69   | 7869              | 142.21               | 1.36        | 121.08  | 0.3                                 |
| 16-Apr-15  | 30.44   | 8273              | 70.17                | 1.45        | 189.92  | 0.39                                |
| 17-Mar-16  | 40.58   | 7941              | 99.12                | 1.33        | 166.29  | 0.29                                |
| 26-Mar-16  | 64.1    | 3291              | 376.76               | 1.29        | 164.62  | 0.17                                |
| 30-Apr-17  | 8.05    | 19 346            | 8.08                 | 1.21        | 216.65  | 1.09                                |
| 3-Feb-18   | 20.04   | 9863              | 39.42                | 1.4         | 196.47  | 0.57                                |
| Wainwright |         |                   |                      |             |         |                                     |
| 21-May-08  | 32.19   | 2889              | 110.32               | 1.33        | 190.65  | 0.16                                |
| 6-Apr-09   | 53.24   | 2185              | 337.67               | 1.71        | 175.58  | 0.19                                |
| 24-May-09  | 73.91   | 2000              | 209.26               | 1.87        | 121.99  | 0.29                                |
| 9-Jul-14   | 32.23   | 93 381            | 14.77                | 1.17        | 75      | 1.41                                |
| 19-Jun-15  | 25.53   | 11 692            | 32.28                | 1.3         | 113.54  | 0.76                                |
| 5-Jul-15   | 1.74    | 2325              | 43.08                | 1.17        | 172.53  | 0.72                                |
| 15-Jun-17  | 5.74    | 3508              | 683.7                | 1.26        | 314.08  | 0.49                                |
| 15-Apr-18  | 44.81   | 8011              | 452.86               | 1.32        | 148.42  | 0.33                                |
| 13-Jul-18  | 27.45   | 9355              | 6.81                 | 1.25        | 133.75  | 0.51                                |

**Table 5** SLI and Wainwright sample size ( $n$ ), correlation ( $R$ ) and  $p$  value for each FRAGSTATS metric versus sea-ice cover. Relationships with  $p < 0.01$  were deemed statistically significant (shown in boldface).

|                | SLI |       |                 | Wainwright |       |                 |
|----------------|-----|-------|-----------------|------------|-------|-----------------|
|                | $n$ | $R$   | $p$             | $n$        | $R$   | $p$             |
| No. of patches | 14  | -0.88 | <b>&lt;0.01</b> | 10         | -0.08 | 0.84            |
| Mean area      | 14  | 0.86  | <b>&lt;0.01</b> | 10         | 0.79  | <b>&lt;0.01</b> |
| ENN            | 14  | -0.77 | <b>&lt;0.01</b> | 10         | -0.37 | 0.29            |
| Shape index    | 14  | 0.14  | 0.64            | 10         | 0.85  | <b>&lt;0.01</b> |
| Edge density   | 14  | -0.86 | <b>&lt;0.01</b> | 10         | -0.46 | 0.18            |

fragmentation characteristics as overall SIC has declined. Both study areas have significant trends in their fragmentation metrics as related to SIC and are experiencing a process of fragmentation based on the decision tree algorithm presented by Bogaert et al. (2004). Walrus require sea-ice conditions that allow easy access to floes and enough open water to perform U-shaped dives while foraging (Jay et al. 2014). The existing literature concludes that walrus are most commonly found on the so-called broken pack (Ray et al. 2010). They utilize areas of fragmented ice and thin ice up to 20 cm thickness,

where they are able to create breathing holes (Burns et al. 1980; Fay 1982; Ray et al. 2010; Jay et al. 2011). We assume that our thick ice category contains sea ice too solid for walrus to break through (>20 cm). Walrus tend to be found in SIC of 20–80% (Fay 1982) and avoid areas with SIC of 90% or more, which would limit their movement in water (Jay et al. 2012). Specific walrus sea-ice preferences and habits are debated in the literature. Ray et al. (2010) state that walrus prefer thick, moderate-sized floes separated by leads and polynyas as a habitat, whilst they are not commonly found in areas of

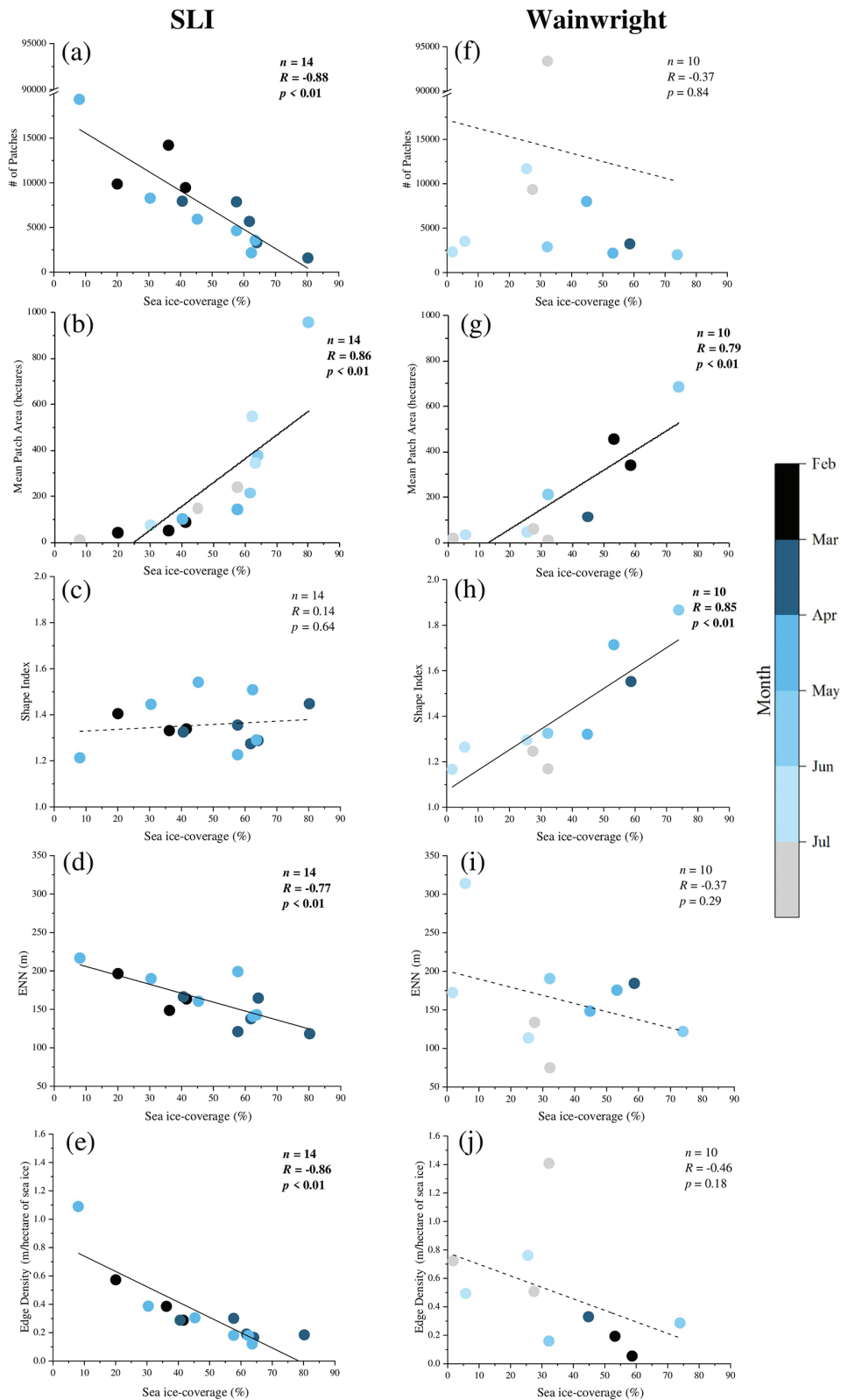


**Fig 5** Scatter plots for both study areas of the five FRAGSTATS metrics versus SIC. Boldface text (and solid trendlines) signifies statistical significance at  $p < 0.01$ . Plots are colour-coded to show general seasonality.

rounded pack (defined as areas of at least 50% heavy ice cover in which floes are founded rather than angular), owing to the lack of open water (Burns et al. 1980; Ray & Hufford 1989; Ray et al. 2010). Additionally, Ray et al. (2006) in 1975 observed that walrus seem to stay close to specific areas of moving ice to feed and return to the same location after feeding (i.e., a 'home' sea-ice area). However, Jay et al. (2010) found that walrus activity was independent of the movement of ice floes, suggesting that they use any available ice conveniently close to their feeding areas. Although walrus' specific preferences and interactions with sea ice may not be clear, the future of sea ice in both study areas will, undoubtedly, show substantial change.

In the Bering Sea, low sea-ice concentrations were associated with significantly more ice floes and edges, less mean floe area and floes that were farther apart. The average distance between floes increased by more than some 50 m as sea-ice coverage declined from 80% to less than 20% thick ice. A study conducted over the years 2005–08 found that walrus migrating across the Davis Strait averaged speeds from 6 to 10 km/hr and travelled an average of 46 km/day (Dietz et al. 2013). This implies that if the distance between floes was to increase an average of 50 m in the Bering, it would not be a particularly long distance to travel for walrus, but this is speculation as current studies do not discuss walrus swimming capabilities. Floe distance increases as SIC decreases in this area because the Bering Sea is conducive to floe movement. For example, sea ice in the Bering forms in the northern portion and can be blown southward by north–north-easterly winds (McNutt 2002). Not being 'land-locked' and having an open sea-ice edge, floes move freely with the wind and currents (Shapiro & Burns 1975). One could speculate that some of these changes may even be beneficial to the Pacific walrus. An increase in floe edges would allow more walrus to haul out along an ice edge, taking advantage of easy access to water without needing to push through densely populated areas. Additionally, the increase in distance from floe to floe and increase in the number of floes could also be helpful to mothers, who usually give birth in semi-isolation on very small floes (<30 m) before joining nursery herds (Fay 1982). Moreover, these increases could create smaller, more dispersed congregations of females during the mating season (January–March), allowing greater movement by males and opening opportunities for other males to mate with females (Fay 1982; Fay et al. 1984). This reduction in inter-male competition could be beneficial in creating a more diverse gene pool (Fay et al. 1984), or conversely, negatively impact sexual selection and fitness (Ray et al. 2016).

In contrast to the Bering Sea results, lower sea-ice concentrations in the Chukchi Sea were associated with a significant decrease in mean ice floe area and more circular floes. More circular floes may not affect walrus if there is open water to feed in. However, although the Chukchi Sea has areas of open water closer to the coast of Alaska, sea ice cannot move as freely as in the Bering Sea (Jay et al. 2010). Chukchi sea ice forms throughout the region and is locked in place for many months, limiting movement (Burns et al. 1980). Without room for movement, ice floes frequently collide and rub against one another, eroding sharp rectangular edges and shaping into overall rounder floes (Burns et al. 1980). This is defined as a rounded pack, in which walrus are not commonly found owing to the lack of open water (Ray et al. 2010). In the future, if rounded pack is more commonly found surrounding productive feeding grounds, the walrus will need to become comfortable foraging in this denser sea-ice pack.

Unsupervised image classification coupled with segmentation classification was a success for this study, having an overall accuracy of 90.75%. Furthermore, it was most accurate at distinguishing between thick ice and water, which was not surprising considering the sharp spectral contrast between the two classes. These results were encouraging because the validation of sea-ice classifications is more difficult for the ever-changing icescapes than landscapes, as it is more challenging to acquire ground-truth observations in the former.

It is arguable that the floe dynamics found in this study are simply a natural progression of seasonal sea-ice melt. As the melting season progresses, we cannot refute that it is natural for sea-ice floes to become more numerous, smaller, farther apart and rounder. One of the side effects of decreasing sea-ice extent is that multi-year ice melts and is replaced with first-year seasonal ice, which is thinner and more vulnerable to melt (Bateson et al. 2020). Oldest ice (more than four years old), which comprised 33% of Arctic Ocean ice pack in 1985, was only 1.2% of the pack in March 2019 (Perovich et al. 2019). The later sea-ice freeze-up and earlier melting periods, coupled with first-year ice, will lead to even earlier fragmentation, creating icescapes with low SIC, and ice-floe dynamics as described in the findings of this study (for the Bering: decreases in mean floe area and increases in floe distance, number of floes and edges; for the Chukchi: decreases in mean floe area and rounder floes). Therefore, this study also has predictive capabilities as lower SIC, in general, will be more common in the future. Future studies could use a less limited satellite (i.e., higher temporal/spatial resolution) to measure seasonal and annual sea-ice dynamics over time in both study areas.

## Conclusions

Future projections estimate that sea ice across the Arctic will continue to decline over the coming decades, which already has substantial impacts on marine species that rely upon it. Less sea ice leads Pacific walrus to use coastal haul-outs more, which is expected to contribute to their decline (MacCracken et al. 2017). This study found that segmentation classification was an accurate way of classifying sea-ice floes, and the assessment of spatial pattern metrics across the two study areas had significant findings. With declining SIC, ice floes in the Chukchi Sea are expected to be smaller and more circular. For the Bering Sea, declining SIC is expected to create scenarios where ice floes are distributed farther apart and are smaller, with more edges. This will lead to longer swimming distances for the walrus and will enhance lateral melting rates in the Bering Sea, whereas in the Chukchi Sea, walrus may be forced to use more circular sea-ice floes if rounded pack is the only option. These changes in sea-ice characteristics may alter the feeding, mating, birthing and migration patterns of Pacific walrus, which could drastically change the ecological role of walrus and have proliferating impacts on benthic ecosystems overall (Ray et al. 2006). This research proves the potential of using landscape fragmentation techniques on icescape environments, filling knowledge gaps as to how sea-ice floe dynamics change as SIC declines. Moreover, this analysis provides the framework of methods necessary to allow future studies to predict how sea-ice fragmentation will directly impact the Pacific walrus and other sea ice-obligate species in the future.

## Acknowledgements

The authors acknowledge Chadwick V. Jay (US Geological Survey, Alaska Science Center) who provided data that were useful in selecting study areas and were also helpful with input regarding the relationship between floe shape and walrus usage. The authors would also like to thank the anonymous reviewers whose comments and suggestions helped to improve and clarify this manuscript.

## Disclosure statement

The authors report no conflict of interest.

## Funding

Funding for this research was provided to KEF by the US National Science Foundation Arctic Observing Network Program (grants OPP-1702137 and OPP-1917434).

## References

- Baker W.L. & Cai Y. 1992. The r.le programs for multiscale analysis of landscape structure using the GRASS geographical information system. *Landscape Ecology* 7, 291–302, doi: 10.1007/BF00131258.
- Bateson A.W., Feltham D.L., Schröder D., Hosekova L., Ridley J.K. & Aksenov Y. 2020. Impact of sea ice floe size distribution on seasonal fragmentation and melt of Arctic sea ice. *The Cryosphere* 14, 403–428, doi: 10.5194/tc-14-403-2020.
- Battaile B., Jay C.V., Udevitz M.S. & Fischbach A.S. 2017. Evaluation of a method using survey counts and tag data to estimate the number of Pacific walrus (*Odobenus rosmarus divergens*) using a coastal haulout in northwestern Alaska. *Polar Biology* 40, 1359–1369, doi: 10.1007/s00300-016-2060-5.
- Bogaert J., Ceulemans R. & Salvador-Van Eysenrode D. 2004. Decision tree algorithm for detection of spatial processes in landscape transformation. *Environmental Management* 33, 62–73, doi: 10.1007/s00267-003-0027-0.
- Burns J.J., Shapiro L.H. & Fay F.H. 1980. *The relationships of marine mammal distributions, densities, and activities to sea ice conditions. Final report.* Boulder, CO: Outer Continental Shelf Environmental Assessment Program, National Oceanic and Atmospheric Administration Environmental Research Laboratory.
- Citta J.J., Lowry L.F., Quakenbush L.T., Kelly B.P., Fischbach A.S., London J.M., Jay C.V., Frost K.J., Crowe G.O., Crawford J.A., Boveng P.L., Cameron M., Von Duyke A.L., Nelson M., Harwood L.A., Richard P., Suydam R., Heide-Jørgensen M.P., Hobbs R.C., Litovka D.I., Marcoux M., Whiting A., Kennedy A.S., George J.C., Orr J. & Gray T. 2018. A multi-species synthesis of satellite telemetry data in the Pacific Arctic (1987–2015): overlap of marine mammal distributions and core use areas. *Synthesis of Arctic Research SOAR Phase II* 152, 132–153, doi: 10.1016/j.dsr.2018.02.006.
- Comiso J.C., Gersten R.A., Stock L.V., Turner J., Perez G.J. & Cho K. 2017. Positive trend in the Antarctic sea ice cover and associated changes in surface temperature. *Journal of Climate* 30, 2251–2267, doi: 10.1175/JCLI-D-16-0408.1.
- Comiso J., Meier W. & Gersten R. 2017. Variability and trends in the Arctic Sea ice cover: results from different techniques. *Journal of Geophysical Research—Oceans* 122, 6883–6900, doi: 10.1002/2017JC012768.
- Didham R.K. 2010. Ecological consequences of habitat fragmentation. In R. Jansson (ed.): *Encyclopedia of life sciences.* A21904, doi: 10.1002/9780470015902.a0021904. Chichester: John Wiley & Sons.
- Dietz R., Born E., Stewart R., Heide-Jørgensen M.P., Stern H., Rigét F., Pedersen L., Lanthier C., Jensen M. & Teilmann J. 2013. *Movements of walrus (Odobenus rosmarus) between central west Greenland and southeast Baffin Island, 2005–2008.* NAMMCO Special Issue 9. Tromsø, Norway: North Atlantic Marine Mammal Commission.
- Douglas D.C. 2010. *Arctic sea ice decline: projected changes in timing and extent of sea ice in the Bering and Chukchi seas.* Open-File Report 2010-1176. Reston, VA: US Geological Survey.

- Drucker R., Martin S. & Moritz R. 2003. Observations of ice thickness and frazil ice in the St. Lawrence Island polynya from satellite imagery, upward looking sonar, and salinity/temperature moorings. *Journal of Geophysical Research—Oceans* 108, article no. 3149, doi: 10.1029/2001JC001213.
- Eastman J.R. 2016. *TerrSet manual*. Worcester, MA: Clark Labs, Clark University.
- Fay F.H. 1982. *Ecology and biology of the Pacific walrus, *Odobenus rosmarus divergens* Illiger*. North American Fauna. Vol. 74. Washington, DC: Fish and Wildlife Service, US Department of the Interior.
- Fay F.H., Ray C.G. & Kibal'chich A.A. 1984. Time and location of mating and associated behavior of the Pacific walrus, *Odobenus rosmarus divergens* Illiger. In F.H. Fay & G.A. Fedoseev (eds.): *Soviet–American cooperative research on marine mammals. Vol. I. Pinnipeds*. NOAA Technical Report NMFS 12. Pp. 81–88. Washington, DC: National Oceanic and Atmospheric Administration, US Department of Commerce.
- Fischbach A.S., Kochnev A.A., Garlich-Miller J.L. & Jay C.V. 2016. Pacific walrus coastal haulout database 1852–2016: US Geological Survey. Alaska Science Center. doi: 10.5066/F7RX994P.
- Franklin J.F. & Forman R.T.T. 1987. Creating landscape patterns by forest cutting: ecological consequences and principles. *Landscape Ecology* 1(1), 5–18.
- Frey K., Comiso J.C., Cooper L.W., Grebmeier J.M. & Stock L.V. 2019. Arctic Ocean primary productivity: the response of marine algae to climate warming and sea ice decline. In J. Richter-Mengde et al. (eds.): *Arctic report card: update for 2019*. Pp. 40–47. Washington, DC: National Oceanic and Atmospheric Administration.
- Hargis C.D., Bissonette J.A. & David J.L. 1998. The behavior of landscape metrics commonly used in the study of habitat fragmentation. *Landscape Ecology* 13(3), 167–186.
- Hauser D.D.W., Laidre K.L. & Stern H.L. 2018. Vulnerability of Arctic marine mammals to vessel traffic in the increasingly ice-free Northwest Passage and Northern Sea Route. *Proceedings of the National Academy of Sciences of the United States of America* 115, 7617–7622, doi: 10.1073/pnas.1803543115.
- Hisabayashi M., Rogan J. & Elmes A. 2017. Quantifying shoreline change in Funafuti Atoll, Tuvalu using a time series of Quickbird, Worldview and Landsat data. *GIScience & Remote Sensing* 55, 307–330, doi: 10.1080/15481603.2017.1367157.
- Jay C.V. & Fischbach A.S. 2008. *Pacific walrus response to Arctic sea ice losses. Fact Sheet 2008–3041*. Anchorage, AK: Alaska Science Center, US Geological Survey. doi: 10.3133/fs20083041.
- Jay C.V., Fischbach A.S. & Kochnev A.A. 2012. Walrus areas of use in the Chukchi Sea during sparse sea ice cover. *Marine Ecology Progress Series* 468, 1–13, doi: 10.3354/meps10057.
- Jay C.V., Grebmeier J.M., Fischbach A.S., McDonald T.L., Cooper L.W. & Hornsby F. 2014. Pacific walrus (*Odobenus rosmarus divergens*) resource selection in the northern Bering Sea. *PLoS One* 9, article no. e93035, doi: 10.1371/journal.pone.0093035.
- Jay C.V., Marcot B.G. & Douglas D.C. 2011. Projected status of the Pacific walrus (*Odobenus rosmarus divergens*) in the twenty-first century. *Polar Biology* 34, 1065–1084, doi: 10.1007/s00300-011-0967-4.
- Jay C.V., Udevitz M.S., Kwok R., Fischbach A.S. & Douglas D.C. 2010. Divergent movements of walrus and sea ice in the northern Bering Sea. *Marine Ecology Progress Series* 407, 293–302, doi: 10.3354/meps08575.
- Kastelein R., Gerrits N.M. & Dubbeldam J.L. 1991. The anatomy of the walrus head (*Odobenus rosmarus*). Part 2: description of the muscles and of their role in feeding and haul-out behaviour. *Aquatic Mammals* 17, 156–180.
- MacCracken J.G. 2012. Pacific walrus and climate change: observations and predictions. *Ecology and Evolution* 2, 2072–2090, doi: 10.1002/ece3.317.
- MacCracken J., Beatty W., Garlich-Miller J., Kissling M. & Snyder J. 2017. *Final species status assessment for the Pacific walrus (*Odobenus rosmarus divergens*), May 2017 (Version 1.0)*. Anchorage, AK: Marine Mammals Management, US Fish & Wildlife Service. doi: 10.13140/RG.2.2.29363.12325.
- McFarland S. & Aerts L. 2015. *Assessing disturbance responses of Pacific walrus (*Odobenus rosmarus divergens*) to vessel presence in the Chukchi Sea*. Anchorage, AK: Chukchi Sea Environmental Studies Program.
- McGarigal K. 2015. *FRAGSTATS help. Version 4.2*. Amherst, MA: University of Massachusetts, Amherst.
- McNutt L. 2002. How does ice cover vary in the Bering Sea from year to year? Accessed on the internet at [https://www.beringclimate.noaa.gov/essays\\_mcnutt.html](https://www.beringclimate.noaa.gov/essays_mcnutt.html) on 9 April 2019.
- Melia N., Haines K. & Hawkins E. 2016. Sea ice decline and 21st century trans-Arctic shipping routes. *Geophysical Research Letters* 43, 9720–9728, doi: 10.1002/2016GL069315.
- Miller M. 2015. *Coast guard maps out marine traffic lanes to the Arctic*. Accessed on the internet at <https://www.ktoo.org/2015/01/27/coast-guard-maps-marine-traffic-lanes-arctic/> on 10 September 2020.
- Monson D.H., Udevitz M.S. & Jay C.V. 2013. Estimating age ratios and size of Pacific walrus herds on coastal haulouts using video imaging. *PLoS One* 8, e69806, doi: 10.1371/journal.pone.0069806.
- Oakley K.L., Whalen M.E., Douglas D.C., Udevitz M.S., Atwood T.C. & Jay C. 2012. *Polar bear and walrus response to the rapid decline in Arctic sea ice. Fact Sheet 2012–3131*. Anchorage, AK: Alaska Science Center, US Geological Survey. doi: 10.3133/fs20123131.
- Overland J.E., Hanna E., Hanssen-Bauer I., Kim S.-J., Walsh J.E., Wang M., Bhatt U.S. & Thoman R.L. 2018. Surface air temperature. In E. Osborne et al. (eds.): *Arctic report card: update for 2018*. Pp. 5–11. Washington, DC: National Oceanic and Atmospheric Administration.
- Perovich D., Meier W., Tschudi M., Farrell S., Hendricks S., Gerland S., Kaleschke L., Ricker R., Tian-Kunze X., Webster M. & Wood K. 2019. Sea ice. In J. Richter-Mengde et al. (eds.): *Arctic report card: update for 2019*. Pp. 26–34. Washington, DC: National Oceanic and Atmospheric Administration.
- Ray G.C. & Hufford G.L. 1989. Relationships among Beringian marine mammals and sea ice. *Rapports et Proces-verbaux des Réunions. Conseil International pour l'Exploration de la Mer* 188, 225–242.
- Ray G.C., Hufford G.L., Overland J.E., Krupnik I., McCormick-Ray J., Frey K. & Labunski E. 2016. Decadal

- Bering Sea seascape change: consequences for Pacific walrus and indigenous hunters. *Ecological Applications* 26, 24–41, doi: 10.1890/15-0430.
- Ray G.C., McCormick-Ray J., Berg P. & Epstein H.E. 2006. Pacific walrus: benthic bioturbator of Beringia. *Journal of Experimental Marine Biology and Ecology* 330, 403–419, doi: 10.1016/j.jembe.2005.12.043.
- Ray G., Overland J. & Hufford G. 2010. Seascape an organizing principle for evaluating walrus and seal sea-ice habitat in Beringia. *Geophysical Research Letters* 37, article no. L20504, doi: 10.1029/2010GL044452.
- Reed R.A., Johnson-Barnard J. & Baker W.L. 1996. Fragmentation of a forested Rocky Mountain landscape, 1950–1993. *Biological Conservation* 75, 267–277, doi: 10.1016/0006-3207(95)00069-0.
- Rösel A. & Kaleschke L. 2011. Comparison of different retrieval techniques for melt ponds on Arctic sea ice from Landsat and MODIS satellite data. *Annals of Glaciology* 52, 185–191, doi: 10.3189/172756411795931606.
- Sacco A. 2015. *Sea-ice habitat preference of the Pacific walrus (Odobenus rosmarus divergens) in the Bering Sea: a multiscaled approach*. MSc thesis, University of Alaska Fairbanks.
- Sahanatien V., Derocher A. & Gompper M. 2012. Monitoring sea ice habitat fragmentation for polar bear conservation. *Animal Conservation* 15, 397–406, doi: 10.1111/j.1469-1795.2012.00529.x.
- Saunders D.A., Hobbs R.J. & Margules C.R. 1991. Biological consequences of ecosystem fragmentation: a review. *Conservation Biology* 5, 18–32, doi: 10.1111/j.1523-1739.1991.tb00384.x.
- Schumacher G.M. 1976a. *Bathymetric map of the Aleutian Trench and Bering Sea. US Geological Survey Open File Report 76-821*. 2 sheets. Accessed on the internet at <https://dggs.alaska.gov/pubs/id/12902> on 9 October 2021.
- Schumacher G.M. 1976b. *Bathymetric map of the Chukchi Sea and Arctic Ocean. US Geological Survey Open File Report 76-823*. 2 sheets. Accessed on the internet at <https://dggs.alaska.gov/pubs/id/12903> on 9 October 2021.
- Shapiro L.H. & Burns J.J. 1975. *Major late-winter features of ice in northern Bering and Chukchi seas as determined from satellite imagery. Sea Grant Report 75-8. Geophysical Institute Report UAG R-236*. Fairbanks, AK: University of Alaska Fairbanks.
- Stabeno P.J. & Bell S.W. 2019. Extreme conditions in the Bering Sea (2017–2018): record-breaking low sea-ice extent. *Geophysical Research Letters* 46, 8952–8959, doi: 10.1029/2019GL083816.
- Stabeno P.J., Thoman R.L. & Wood L. 2019. Recent warming in the Bering Sea and its impact on the ecosystem. In J. Richter-Mengde et al. (eds.): *Arctic report card: update for 2019*. Pp. 81–87. Washington, DC: National Oceanic and Atmospheric Administration.
- Stroeve J.C., Markus T., Boisvert L., Miller J. & Barrett A. 2014. Changes in Arctic melt season and implications for sea ice loss. *Geophysical Research Letters* 41, 1216–1225, doi: 10.1002/2013GL058951.
- Taylor R.L., Udevitz M.S., Jay C.V., Citta J.J., Quakenbush L.T., Lemons P.R. & Snyder J.A. 2018. Demography of the Pacific walrus (*Odobenus rosmarus divergens*) in a changing Arctic. *Marine Mammal Science* 34, 54–86, doi: 10.1111/mms.12434.
- Turner M., Gardner R. & O'Neill R. 2003. *Landscape ecology in theory and practice: pattern and process*. New York: Springer.
- Udevitz M.S., Jay C.V., Taylor R.L., Fischbach A.S., Beatty W.S. & Noren S.R. 2017. Forecasting consequences of changing sea ice availability for Pacific walrus. *Ecosphere* 8, e02014, doi: 10.1002/ecs2.2014.
- US Fish & Wildlife Service 2017. *12-month findings on petitions to list 25 species as endangered or threatened species*. Accessed on the internet at <https://ecos.fws.gov/ecp/species/8791> on 8 April 2019.
- USGS (US Geological Survey) 2017. *Landsat 7*. Accessed on the internet at <https://earthexplorer.usgs.gov/> on 15 April 2019.
- USGS (US Geological Survey) 2018. *Landsat Shapefiles and KML Files*. Accessed on the internet at <https://www.usgs.gov/landsat-missions/landsat-shapefiles-and-kml-files> on 15 November 2018.
- Wartzok D. & Ray G.C. 1980. *The hauling-out behavior of the Pacific walrus. Report of the U.S. Marine Mammal Commission. PB 80-192 578*. Springfield, VA: National Technical Information Service.